

# Morphological enhancement of microscopy mineral image using opening- and closing-based toggle operator

X. BAI\*,†,‡

\*Image Processing Center, Beijing University of Aeronautics and Astronautics

†State Key Laboratory of Virtual Reality Technology and Systems

‡Beijing Key Laboratory of Digital Media, Beihang University, Beijing, 100191, China

**Key words.** Mineral image enhancement, toggle operator, opening, closing, mathematical morphology, microscopy image analysis.

## Summary

To enhance unclear microscopy mineral images, an algorithm based on toggle operator using opening and closing is proposed in this paper. Firstly, the specified toggle operator using opening and closing through designing the selection rules is analysed. Secondly, after importing the multiscale theory into the specified toggle operator, useful mineral image features, especially the mineral details, are extracted using the multiscale theory-based toggle operator. Finally, the mineral image is enhanced through the strategy of enlarging the contrast between the extracted bright and dark image features. Experimental results on different types of mineral images verified that the proposed algorithm could effectively enhance mineral images and performed better than some other algorithms. The enhanced mineral image is clear and contains rich mineral details, whereas the grey scale distribution of the original mineral image is appropriately maintained. This would be useful for the further mineral analysis. Therefore, the proposed algorithm could be widely used for image-based mineral applications.

## Introduction

Microscopy imaging has been an important tool in the mineral analysis. Mineral images obtained by scanning electron microscopy, transmission electron microscopy, scanning tunneling microscopy and some other microscopy equipment may be not clear because of the microscopy imaging equipment or equipment operators (Carter *et al.*, 2000; Fürhapter *et al.*, 2005; Cheng *et al.*, 2006; Yew & Sheppard, 2006; Poulikakos & Partl, 2010). So, enhancing mineral image would be important for mineral applications. Improving the imaging procedure during operation of the microscope or using a higher

specification microscope is the best way (Poulikakos & Partl, 2010). However, enhancing the obtained images would be a more direct and feasible way if the images have been already obtained. Image enhancement has been a useful tool for image-based applications (Foracchia *et al.*, 2005; Bai *et al.*, 2009; Tru *et al.*, 2009; Bai and Zhou, 2011; Bai *et al.*, 2011). Different algorithms have been proposed for image enhancement. Histogram-based algorithms (Huang *et al.*, 2006; Wan & Shi, 2007) are one type that is widely used. However, some histogram-based algorithms may over enhance the bright regions, which may suppress some important mineral image details in these regions. Diffusion-based algorithms (Tang *et al.*, 2001; Guy *et al.*, 2004) are also effective for image enhancement, which are mainly used for images with noise. Transforming image into other domains, such as the frequency domain (Hayit *et al.*, 2000; Sos *et al.*, 2001) or wavelet domain (Yang & Hansell, 1997; Arianna *et al.*, 2008), is a good way to extract the useful image features for enhancement. But some information may be lost in the transformation, which may affect the performance of image enhancement. Mathematical tools, such as fuzzy logic (Youngsik & Raghu, 1997; Farzam *et al.*, 2000; Yang *et al.*, 2008) and filters (Bruce & Eric, 1999; Foracchia *et al.*, 2005), have been tried to enhance images. However, most of these algorithms perform well for images with noise, which may be inappropriate for mineral image enhancement.

Mathematical morphology has been an important theory in image processing (Serra, 1988; Shavemaker *et al.*, 2000; Soille, 2003; Dorini & Leite, 2007). Morphological operators are widely used in different image-based applications, including image enhancement. Top-hat transform could extract image features and then enhance images through enhancing the image features (Mukhopadhyay & Chanda, 2000; Bai & Zhou, 2010a, b). However, top-hat transform may import noise into the final result image if the image features could not be effectively used. The grey scale distribution of the original image, which usually represents the visual effect of different

Correspondence to: Xiangzhi Bai, Image Processing Center, Beijing University of Aeronautics and Astronautics, Beijing 100191, China. Tel.: +861082338578; fax: +86-10-82316502; e-mail: jackybxz163@163.com

image regions and is the important observing information in mineral images, may also be apparently changed. This will affect the application of the enhanced image for the further mineral analysis. Toggle operator could enhance image details and maintain the grey scale distribution of the original mineral image (Soille, 2003; Maragos, 2005; Bai & Zhou, 2011), which may be appropriately used for mineral image enhancement. However, using the original toggle operator based on dilation and erosion operators may change the sizes of mineral image regions (Bai & Zhou, 2011), which may smooth some image details and affect the quantitative mineral analysis.

To keep the original information of the mineral image, the enhancement algorithm should make the original mineral image clear and make the invisible mineral image details visible while ensuring that the grey scale distribution should not be apparently changed. In fact, morphological opening and closing operators could smooth image features (Soille, 2003; Bai & Zhou, 2010a), which may be used for mineral image feature identification. Moreover, toggle operator could selectively output image features identified by the defined operators following the specified selection rules (Soille, 2003; Maragos, 2005). So, using opening and closing and designing the selection rules will produce a good tool for extracting the important mineral features. Based on the extracted image features, effective mineral image enhancement algorithm may be constructed to maintain the grey scale distribution of the mineral image and make the mineral image clear.

In light of this, a mineral image enhancement algorithm using the opening and closing-based toggle operator is proposed in this paper. The toggle operator is specified through designing the selection rules and using opening and closing, which could be used for extracting the useful mineral image features. After that, the extraction of bright and dark mineral image features is discussed. The multiscale theory using multiscale structuring elements is also given to extract the useful mineral image features and details at different scales of image. Finally, the mineral image is effectively enhanced by using the strategy of contrast enlargement. Experimental results verified that the proposed algorithm could be effectively used for mineral image enhancement and maintaining the grey scale distribution of the original mineral image. The performance is better than some other algorithms. Therefore, the proposed algorithm is an effective way for mineral image enhancement and could be used for mineral image-based applications such as the mineral property analysis, mineral identification and inter-action analysis between minerals and bacteria. For instance, effectively enhanced mineral images are very helpful for exploiting the mechanism of the interactions between the minerals and bacteria contained in the image (Li *et al.*, 2012), which are the important data for accurately explaining the new findings in geomicrobiology area.

## Material and methods

### Mathematical morphology

Mathematical morphology is an important theory in image processing and pattern recognition (Serra, 1988; Shavemaker *et al.*, 2000; Soille, 2003; Dorini & Leite, 2007). Morphological operators have been widely used in different applications. Suppose  $f$  is the original image.  $B$  is the structuring element used in morphological operators. Two basic morphological operators, dilation and erosion, are defined as follows:

$$f \oplus B(x, y) = \max_{u,v} (f(x-u, y-v) + B(u, v)),$$

$$f \ominus B(x, y) = \min_{u,v} (f(x-u, y-v) + B(u, v)),$$

$(x, y)$  and  $(u, v)$  represent the pixel coordinates of  $f$  and  $B$ , respectively.  $\oplus$  and  $\ominus$  are the dilation and erosion operators, respectively.

Based on dilation and erosion, the opening and closing, denoted by  $f \circ B$  and  $f \bullet B$ , are defined as follows:

$$f \circ B = (f \ominus B) \oplus B,$$

$$f \bullet B = (f \oplus B) \ominus B.$$

Opening could be used to smooth bright image features, and closing smooths dark image features.

### Toggle operator

Toggle operators are defined based on other morphological operators and selection rules. One definition of toggle operator is given as follows (Soille, 2003; Maragos, 2005).

$$TO(f)(x, y) = \begin{cases} f_1(x, y), & \text{if } f_2(x, y) - f(x, y) < f(x, y) - f_1(x, y) \\ f_2(x, y), & \text{if } f_2(x, y) - f(x, y) > f(x, y) - f_1(x, y) \\ f(x, y), & \text{else} \end{cases}$$

$f_1(x, y)$  and  $f_2(x, y)$  are the results of the used operators. In this definition, the value of toggle operator  $TO$  at any pixel is selected from the result of the used operator  $f_1(x, y)$  or  $f_2(x, y)$ , which is more different from the value of the same pixel in the original image  $f(x, y)$ . These pixels are the important image features in the mineral image. Therefore, this definition would be very useful for identifying the mineral image features.

### Opening and closing-based toggle operator

It is crucial to effectively identify the important image features for mineral image enhancement. Toggle operator could selectively identify image features following different rules. Also, carefully defining the operators in the toggle operator would

be helpful for feature extraction. So, constructing toggle operator following this way would produce effective operators for identifying image features.

Opening and closing smooth bright and dark image features will change the grey values of pixels, which contain grey values indicating the useful image features. So, opening and closing operators could be used in toggle operator for extracting mineral image features. Based on the analysis above, the opening and closing-based toggle operator is defined as follows:

$$TO(f)(x, y) = \begin{cases} f \circ B(x, y), & \text{if } f \bullet B(x, y) - f(x, y) < f(x, y) - f \circ B(x, y) \\ f \bullet B(x, y), & \text{if } f \bullet B(x, y) - f(x, y) > f(x, y) - f \circ B(x, y) \\ f(x, y), & \text{else.} \end{cases}$$

#### Analysis of the decision rules

The grey value changing of one pixel after opening or closing operator may be different. If the grey value changing of one pixel after opening is larger than the grey value changing of one pixel after closing, the corresponding pixel represents the important bright image feature. Otherwise, the corresponding pixel represents the important dark image feature. So, the important mineral image features could be identified through comparing the grey value changing after opening and closing as the definition of  $TO$  shows. This definition indicates that the identified image features by opening or closing have larger grey value changes. So, the identified image features would be more effective for the feature extraction in the mineral image.

#### Feature extraction

The pixels with changed grey values produced by opening operator represent the bright mineral image features selected using toggle operator, which could be extracted through comparing the grey values of the original image and the result of toggle operator as follows:

$$BTO(f)(x, y) = \max(f(x, y) - TO(f)(x, y), 0),$$

$BTO$  represents the extracted bright mineral image features. These bright image features are the useful image features with large grey values comparing with the surrounding regions in the original image. Similarly, the pixels with changed grey values produced by closing operator, which represent the dark image features, could be extracted as follows:

$$DTO(f)(x, y) = \max(TO(f)(x, y) - f(x, y), 0),$$

$DTO$  represents the extracted dark mineral image features with small grey values in the original mineral image.

Because of the selection by the toggle operator, the extracted bright and dark image features are the clear image features in mineral image. Enhancing these image features is very important for mineral image enhancement and would effectively make the image clear.

#### Multiscale feature extraction

Opening and closing smooth image features corresponding to the scale specified by the size of the used structuring element  $B$ . The content of a mineral image usually has different sizes, which means the image contains features at different scales. To effectively enhance mineral image, the multiscale image features existed at all the scales should be extracted (Jackway & Deriche, 1996; Oliveira & Leite, 2008; Bai & Zhou, 2011). To achieve this purpose, multiscale structuring elements with different sizes should be used. Let  $B_1, \dots, B_n$  represent the  $n$  scales of structuring elements which have the same shape and increasing sizes.  $B_i = \underbrace{B_1 \oplus B_1 \dots \oplus B_1}_{\text{dilation } i \text{ times}}, 1 \leq i \leq n$ . Based on the multiscale structuring element  $B_i$  at scale  $i$ , the multiscale specified toggle operator using opening and closing is expressed as follows:

$$TO(f)(x, y) = \begin{cases} f \circ B_i(x, y), & \text{if } f \bullet B_i(x, y) - f(x, y) < f(x, y) - f \circ B_i(x, y) \\ f \bullet B_i(x, y), & \text{if } f \bullet B_i(x, y) - f(x, y) > f(x, y) - f \circ B_i(x, y) \\ f(x, y), & \text{else.} \end{cases}$$

Based on the multiscale expression of toggle operator, the bright and dark important mineral image features at each scale  $i$ , denoted by  $BTO_i$  and  $DTO_i$ , could be extracted as follows, respectively.

$$BTO_i(f)(x, y) = \max(f(x, y) - TO_i(f)(x, y), 0),$$

$$DTO_i(f)(x, y) = \max(TO_i(f)(x, y) - f(x, y), 0).$$

These extracted multiscale bright and dark mineral image features represent the important information contained in the original mineral image. Therefore, through utilizing these extracted image features, the mineral image may be effectively enhanced.

Figure 1 is an example of a mineral image. The image is not clear. In particular, some important information in the original image, such as the contour information of some image regions and details, are not very clear. Figure 2 lists the extracted bright image features (1) and dark image features (2) corresponding to the third scale. To appropriately show the images, the grey scale distribution of the two feature images are refined in  $[0, 100]$ . These figures clearly show that the extracted mineral image features contain the important contour and detail information which could be used for mineral image enhancement.

#### Mineral image enhancement

The grey values of the extracted bright mineral image features in  $BTO$  are large grey values at different scales. So, the final bright mineral image features of all the scales, denoted by



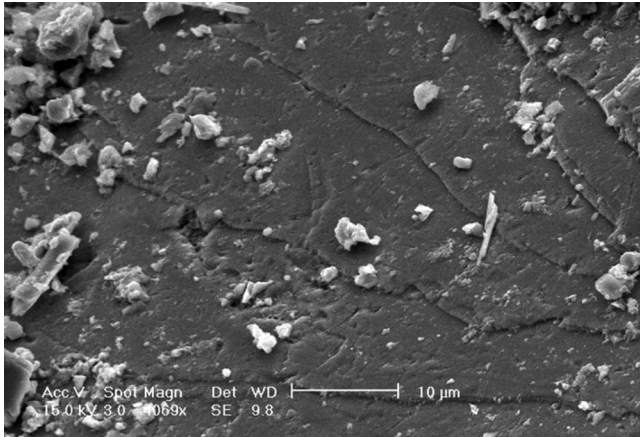


Fig. 1. Original mineral image observed under scanning electron microscopy (SEM). The SEM was operated at an accelerating voltage of 15.0 kV and a magnification of 4069 $\times$ . The spot size was 3.0 mm. The working distance between the specimen surface and the objective lens was 9.8 mm. The main field of view was a natural mineral particle of sphalerite, which was covered by some particles with smaller size.

$BF$ , should be the pixel-wise maximum of the extracted bright mineral image features of all the scales as follows:

$$BF(x, y) = \max_i (BTO_i(f)(x, y)).$$

Similarly, the final dark mineral image features of all the scales, denoted by  $DF$ , could be also obtained as follows:

$$DF(x, y) = \max_i (DTO_i(f)(x, y)).$$

The final extracted bright mineral image features  $BF$  represent the important bright image regions in the original image, and the final extracted dark image features  $DF$  represent the dark image regions in the original image. The direct way of image enhancement is the strategy of enlarging the contrast between the bright and dark image regions through adding the bright image regions on and subtracting the dark image regions from the original mineral image as follows:

$$RI(x, y) = f(x, y) + w_1 \times BF(x, y) - w_2 \times DF(x, y),$$

$RI$  represents the final enhanced image.  $w_1$  and  $w_2$  are positive weights to adjust the contrast of the final result image. This strategy of contrast enhancement through enlarging the differences between the bright and dark image features has been recognized as the effectively and widely used way for image enhancement (Mukhopadhyay & Chanda 2000; Soill, 2003).

In the final enhanced image  $RI$ , the bright image features are enhanced because the bright image features  $BF$  are added on the original image  $f$ . Also, the dark image features are enhanced through subtracting the dark image features  $DF$  from the original image  $f$ . So, the original mineral image would be clear. Moreover, this strategy of enhancement ensures that the bright or dark image regions of the original mineral image regions are still bright or dark in the final enhanced image. So, the grey scale distribution of the original mineral image is appropriately maintained, which would be benefit for the analysis of the enhanced image. All of these ensure that the proposed algorithm could be effectively used for mineral image enhancement.

#### Parameter selection

The main parameters used in this paper are the structuring element, scale number  $n$  and positive weights  $w_1$  and  $w_2$ .

Structuring element is the important parameter in mathematical morphology-based algorithms. The widely used structuring element is the flat structuring element which could be decided by only defining the shape and size of the structuring element. The widely used shapes are rectangle, square, rhombus and circle. Because the circle structuring element has no sharp corners, using circle shape may suppress some produced block effect, so this shape was used in this paper. The size of the structuring element at each scale corresponds to the size of each scale.

The scale number  $n$  decides the extracted image features. Using large scale number could extract more image features at more scales, which may be good for mineral image enhancement. However, experimental results show that there is no need to use a very large scale number, and a very large scale number may apparently increase the calculation time of the

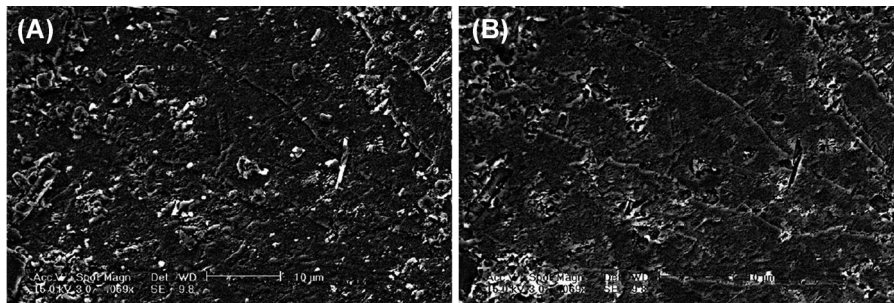
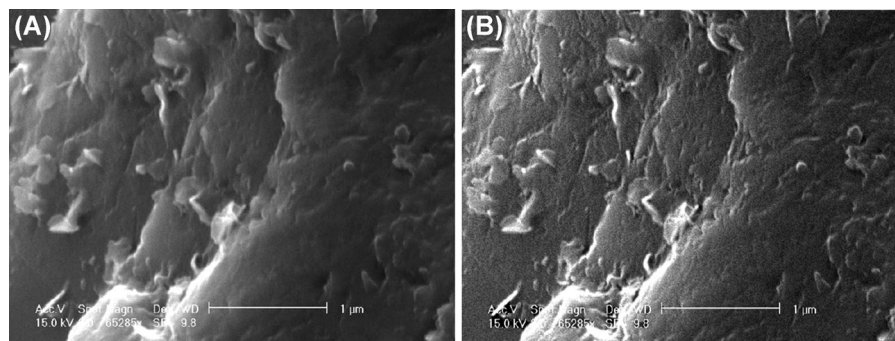
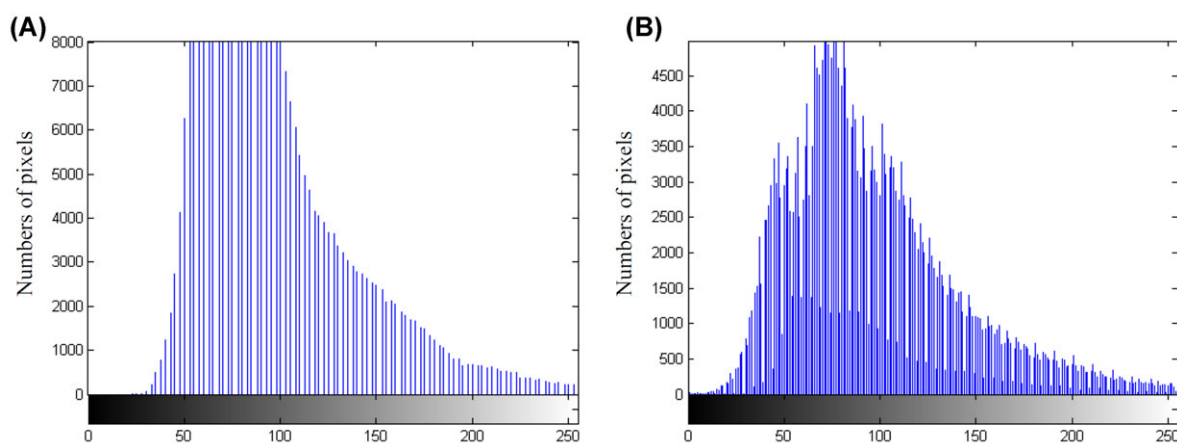


Fig. 2. Bright (A) and dark (B) features at scale 3.



**Fig. 3.** An example of mineral image enhancement. (A) is the original image under scanning electron microscopy (SEM). The SEM was operated at an accelerating voltage of 15.0 kV and a magnification of 65285 $\times$ . The spot size was 3.0 mm. The working distance between the specimen surface and the objective lens was 9.8 mm. The main field of view was a natural mineral particle of sphalerite. (B) is the enhanced result by the proposed algorithm.



**Fig. 4.** Histograms corresponding to the images shown in Figure 3. (A) Histogram of the original image; (B) Histogram of the enhanced result.

proposed algorithm. Experiments on different types of mineral images suggested that using scale number  $n = 3 \sim 5$  would be effective. Therefore, we set  $n = 3$  in this paper.

Note that  $w_1$  and  $w_2$  are positive weights to adjust the enhancement effect of the final result image. To maintain the grey scale distribution of the original mineral image in the final enhanced image,  $w_1$  and  $w_2$  should not be very large. Experimental results show that setting  $w_1 = w_2 = 1.0$  is effective for mineral image enhancement.

## Results and discussions

To verify the good performance of the proposed algorithm, four real data sets containing 100 mineral images were used in this paper, taken from Bai & Zhou (2011). The images are obtained using different microscopes, including the scanning electron microscopy and environmental scanning electron microscopy. Also, the accelerating voltage, magnification, working distance and spot size used in the microscopy when producing the mineral images are different. These images contain different types of minerals for different applications.

Figure 3 is an example of mineral image enhancement, (A) is the original image and (B) is the enhanced result by the proposed algorithm. The original image is not clear with weak image details. After the enhancement, the image becomes clearer. The contours of the mineral edges are clear, and the contained visible image details are rich. To demonstrate the good performance of the proposed algorithm for maintaining the grey scale distribution, the histograms of the original mineral image and the enhanced mineral image in Figure 3 are shown in Figure 4. Figure 4 shows that the profile of the histogram of the enhanced image is very similar as the profile of the original image. Moreover, it could be observed from the original and enhanced mineral images in Figure 3 that the image regions that are bright or dark regions in the original mineral image are still bright or dark in the enhanced result. This would be important for the further mineral analysis. Moreover, the histogram of the original mineral image is very sparse, whereas the histogram of the enhanced image is dense. This indicates that the image details are effectively enhanced, which makes the grey levels rich.

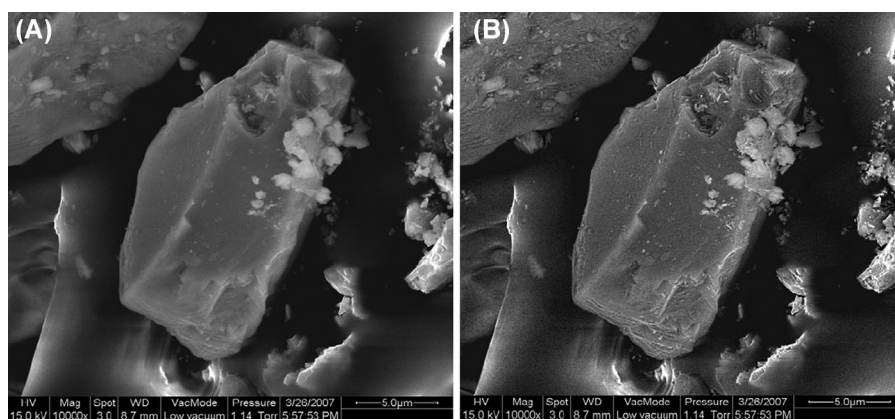


Fig. 5. Example of unclear mineral image enhancement. (A) is the original image under environmental scanning electron microscopy (ESEM). The ESEM was operated at an accelerating voltage of 15.0 kV and a magnification of 10000 $\times$ . The spot size was 3.0 mm. The working distance between the specimen surface and the objective lens was 8.7 mm. The main field of view was a natural mineral particle of sphalerite, which was covered by some particles with smaller size. (B) is the enhanced result by the proposed algorithm.

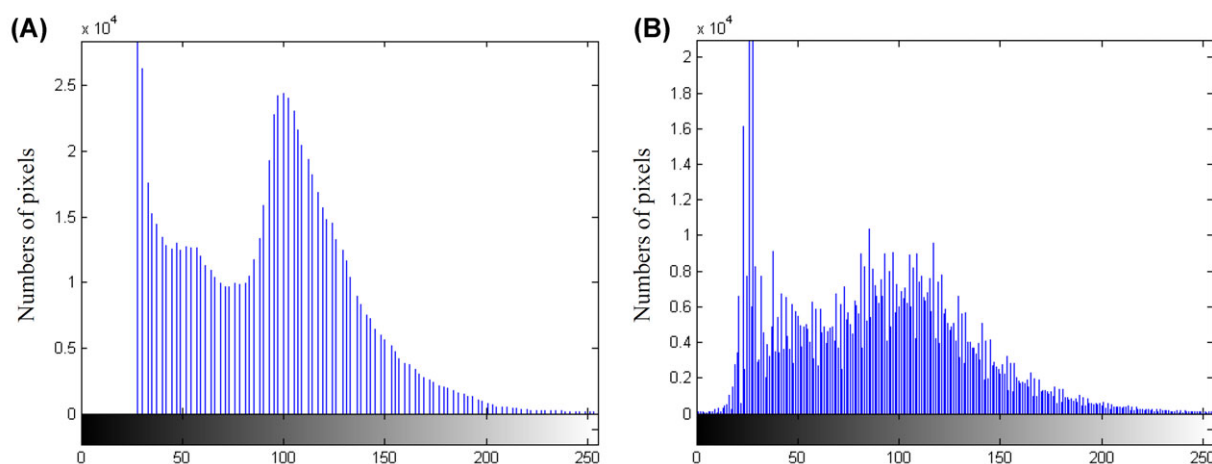


Fig. 6. Histograms corresponding to the images shown in Figure 5. (A) Histogram of the original image; (B) Histogram of the enhanced result.

Figure 5 is the example of unclear mineral image enhancement. (A) is the original mineral image, which is not clear. (B) is the enhanced result by the proposed algorithm. The details in the mineral regions (Fig. 5A) are not visible. After the enhancement, the mineral image is very clear. Also, the histograms of the original mineral image and the enhanced mineral image in Figure 5 are shown in Figure 6. Similar to the results shown in Figures 3 and 4, the profile of the histogram of the enhanced image is similar to the profile of the original image. The bright or dark regions of the original mineral image are still bright or dark in the enhanced mineral image. These indicate that the grey scale distribution of the mineral image is maintained. And, the histogram of the enhanced mineral image is denser than the original mineral image, which verifies the good performance of the proposed algorithm for mineral image enhancement.

Different published algorithms were used to compare outcomes, such as the classical toggle operator-based algorithm

(CTO) (Bai and Zhou, 2011), multiscale morphological approach (MSM) (Mukhopadhyay & Chanda, 2000), Wallis filter algorithm (WF) (Foracchia *et al.*, 2005), histogram equalization algorithm (HE) (Wan & Shi, 2007) and contrast limited adaptive histogram equalization algorithm (CLAHE) (Huang *et al.*, 2006). CTO is a classical toggle operator-based algorithm to enhance mineral images. MSM is a multiscale morphological algorithm which is based on the classical opening and closing operators, and MSM has been verified as the effective algorithm for enhancing different types of images. WF is an effective filter-based image enhancement algorithm. HE and CLAHE are the widely used histogram-based algorithms which are important classes of image enhancement algorithms and could be used for mineral image enhancement. The proposed algorithm is a MSM toggle operator-based algorithm and the performance is effective.

Figure 7 is a comparison example of mineral image enhancement with unclear and rich image details. (A) is the original



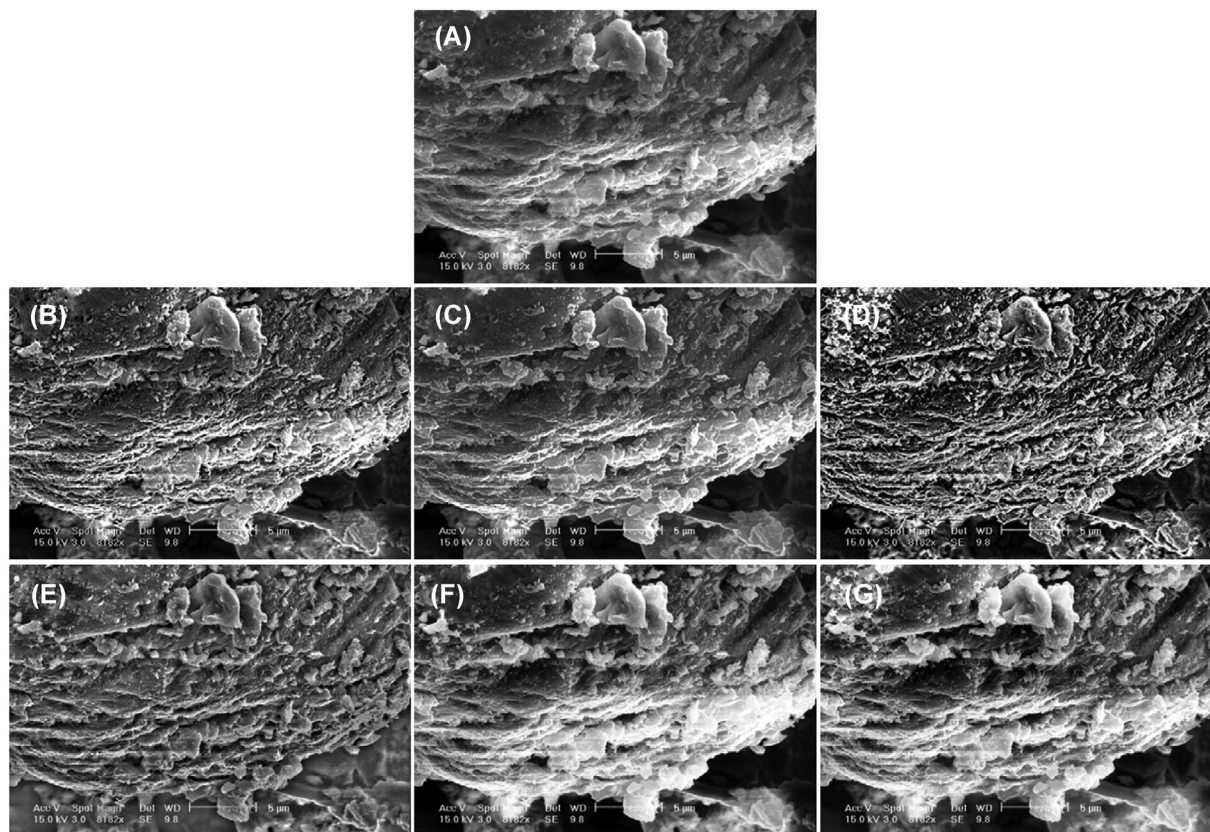


**Fig. 7.** Comparison result. (A) Original image under scanning electron microscopy (SEM). The SEM was operated at an accelerating voltage of 15.0 kV and a magnification of 8182 $\times$ . The spot size was 3.0 mm. The working distance between the specimen surface and the objective lens was 9.8 mm. The main field of view was a natural mineral particle of sphalerite covered by many particles with smaller size; (B) Enhanced result by the proposed algorithm; (C) Enhanced result by CTO; (D) Enhanced result by MSM; (E) Enhanced result by WF; (F) Enhanced result by HE; (G) Enhanced result by CLAHE.

mineral image; (B) is the enhanced result of the proposed algorithm; (C) is the enhanced result of CTO. (D) is the enhanced result of MSM; (E) is the enhanced result of WF; (F) is the enhanced result of HE; (G) is the enhanced result of CLAHE. The original mineral image contains rich image details, which are not clear and there are some bright image regions. WF apparently changes the grey scale distribution of the original mineral image. This may heavily affect the mineral analysis. HE and CLAHE over enhance the bright regions, and image details in these regions are smoothed. MSM enhances the original mineral image, and the details in the original image are clear. However, MSM also changes the grey scale distribution of the original mineral image and produces noise, which may affect the application of the enhanced image. Although CTO enhances image details and the enhanced image is clear, some image details are still smoothed. The proposed algorithm effectively enhances the mineral regions in the original image and the image details are clear. Also, the grey scale distribution is appropriately maintained. **Therefore, the proposed algorithm performs better than other algorithms for mineral image enhancement.**

To quantitatively demonstrate the good performance of the proposed algorithm, the histograms of the original and enhanced mineral images of different algorithms on the example corresponding to Figure 7 are shown in Figure 8. In Figure 8, (A) is the histogram of the original mineral image corresponding to Figures 7(A–G) are the histograms of the enhanced mineral images by the proposed algorithm, CTO, MSM, WF, HE and CLAHE corresponding to Figure 7, respectively. Figure 8 shows that the histogram of the original mineral image is not dense, i.e. some grey levels are missing, so that the original mineral image is not clear. Also, the profile of the histogram has a large slope, which limits the number of grey levels. Thus, the contrast is not good. The histogram of the enhanced result by HE is even sparse compared with the original mineral image. This is because many image regions are over enhanced and the image details are smoothed. The histogram of the enhanced result by CLAHE is dense and does not have sharp slope. So, the contrast is better than the result of HE, but, CLAHE also smooths some image details and the result is still not clear. The histogram of the enhanced result by WF is dense, which means each grey level has useful information in

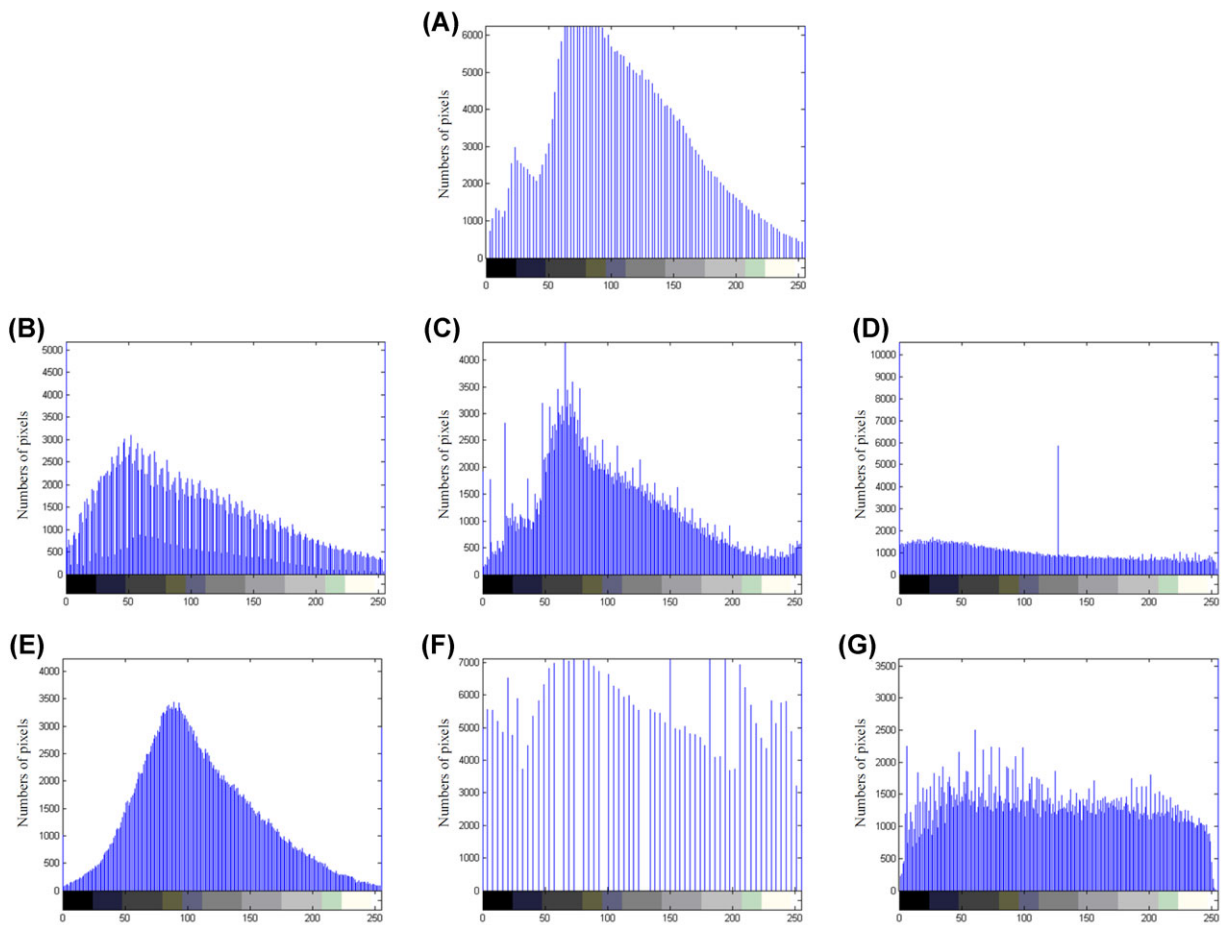


**Fig. 8.** Histogram comparison result corresponding to the images shown in Figure 7. (A) Histogram of the original image; (B) Histogram of the proposed algorithm; (C) Histogram of CTO; (D) Histogram of MSM; (E) Histogram of WF; (F) Histogram of HE; (G) Histogram of CLAHE.

the enhanced image. So, some image details are clear. However, because the profile of the histogram has sharp slope, the enhancement is not effective. The histogram of the enhanced result by MSM is dense. The slope of the profile is small, so the image details are well enhanced and the contrast is good. However, there is a high value at a grey level (see the highest vertical line in Fig. 8 D), which may represent the produced noise in the enhanced image. The histogram of the enhanced result by CTO is dense, which indicates a clear image with well enhanced image details. Also, the slope of the profile of the histogram is still such sharp that the contrast may not be very good. The histogram of the enhanced result by the proposed algorithm is dense and the profile does not have very sharp slope. These mean the image details are effectively enhanced and the contrast is good. Moreover, there are two observed profiles in the histogram, which is interesting. This may be because the image details at each grey level are effectively enhanced by the proposed algorithm. So, the image details are clear in the enhanced image. Therefore, the proposed algorithm performs well for mineral image enhancement and the

enhanced result is clear. Moreover, the performance is better than some other algorithms.

To do the further quantitative comparisons, some well used measures, including the peak signal-to-noise ratio (PSNR), spatial frequency (SF) (Peli, *et al.*, 1994; Aslantas & Kurban, 2009) and mean gradient (MG) (Pradham, *et al.*, 2008; Sheet, *et al.*, 2010), are used in this paper. It is difficult to accurately quantify the performance of image enhancement algorithm using only one measure. Mineral image contains rich image details and spatial information. Enhancing the mineral image should enhance the image details and spatial information. Meanwhile, the possibly produced noise should be suppressed. Therefore, we use PSNR, SF and MG to quantify the produced noise, spatial information and contained image details of the enhanced mineral image of each algorithm, which may give the appropriate evaluations of the mineral image enhancement algorithms. PSNR has been well used to quantify the produced noise in images. SF is a widely used measure defining based on the spatial information of images. MG, which is defined based on image gradient, could be used to quantify the



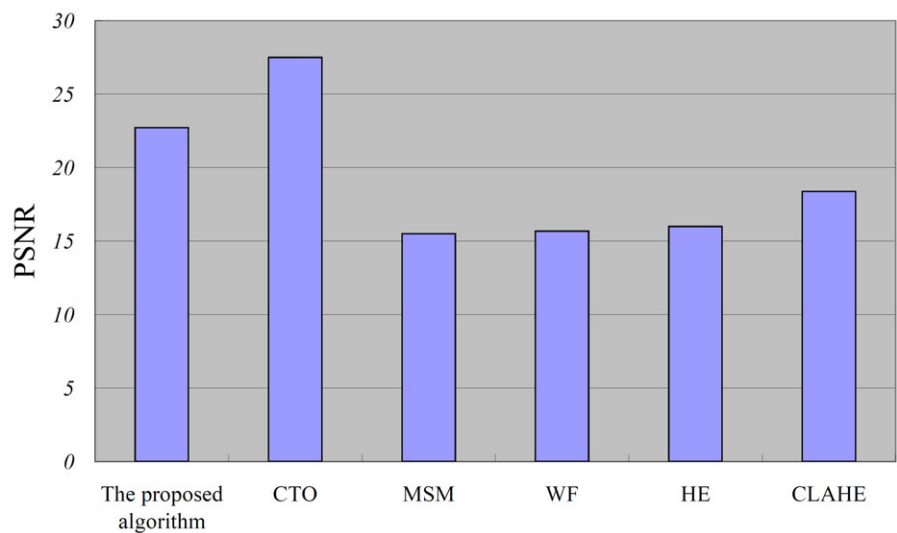


Fig. 9. Quantitative comparison using measure PSNR.

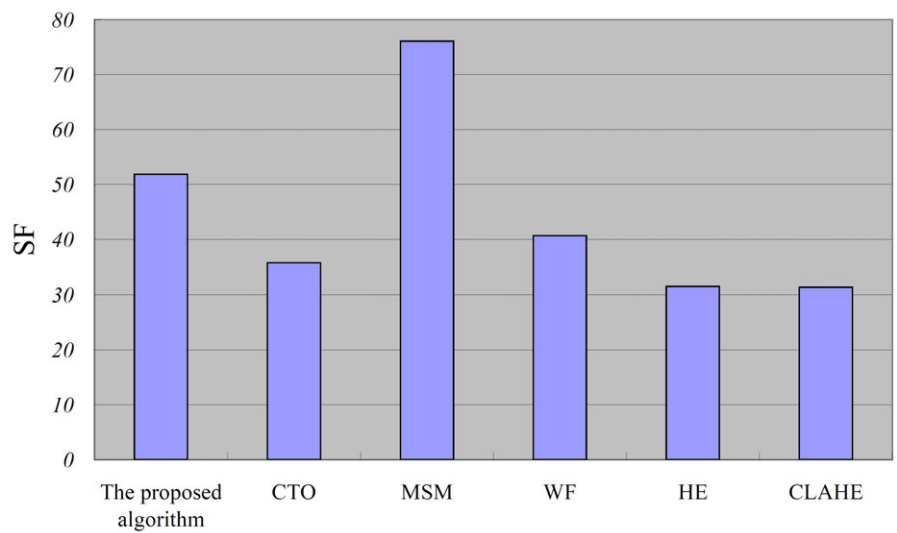


Fig. 10. Quantitative comparison using measure SF.

contained image details. Thus, PSNR, SF and MG are used in this paper. Large values of PSNR, SF and MG indicate good performance of the corresponding mineral image enhancement algorithm.

Mineral images from the four image sets are processed by each algorithm. The PSNR, SF and MG values of the enhanced images corresponding to each algorithm are calculated, respectively. The mean value of the values of each measure corresponding to each algorithm is shown in Figures 9–11, respectively.

Figure 9 is the comparison of the algorithms using measure PSNR. Figure 10 is the comparison of the algorithms using measure SF. Figure 11 is the comparison of the algorithms using measure MG. Figures 9–11 show that the values of WF,

HE and CLAHE are small, which indicates that they may produce heavy noise in the enhanced image and could not well enhance the mineral image details and spatial information. The values of SF and MG of MSM are large, which verified that MSM could enhance the mineral image details and spatial information. However, the value of PSNR of MSM is the smallest. This further verifies that MSM would produce excessive noise in the enhanced image which has been already verified in the visual comparisons in Figure 7. CTO has the largest PSNR value. However, the values of SF and MG of CTO are small. This indicates that the CTO could effectively suppress the produced noise in the result image, but the image details and spatial information are not effectively enhanced. In Figures 9–11, although the value of the proposed algorithm

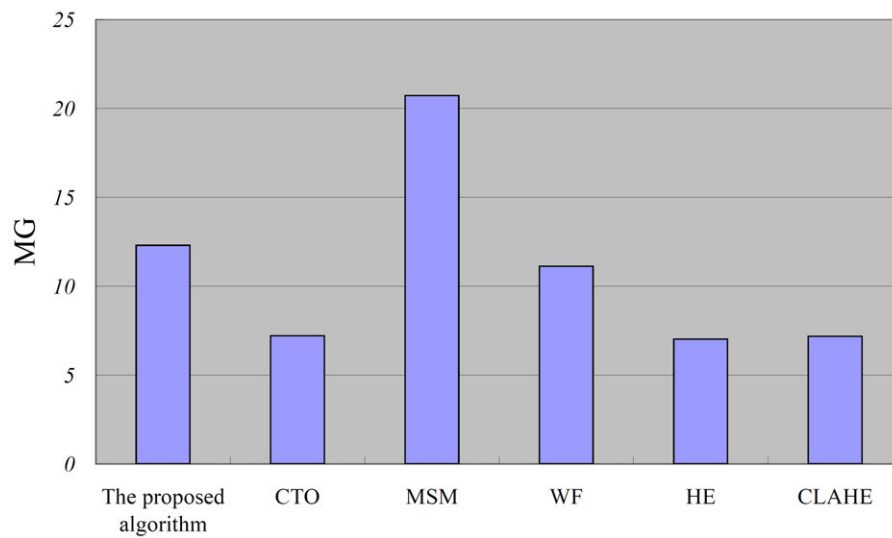


Fig. 11. Quantitative comparison using measure MG.

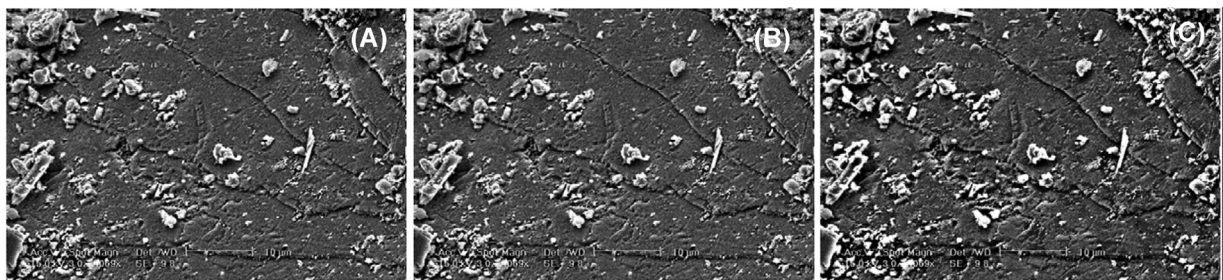


Fig. 12. Enhanced results of the proposed algorithm using different scale numbers and weights  $w_1 = w_2 = 1.0$  on one example mineral image. (A) Enhanced results with scale number  $n = 3$ ; (B) Enhanced results with scale number  $n = 4$ ; (C) Enhanced results with scale number  $n = 5$ .

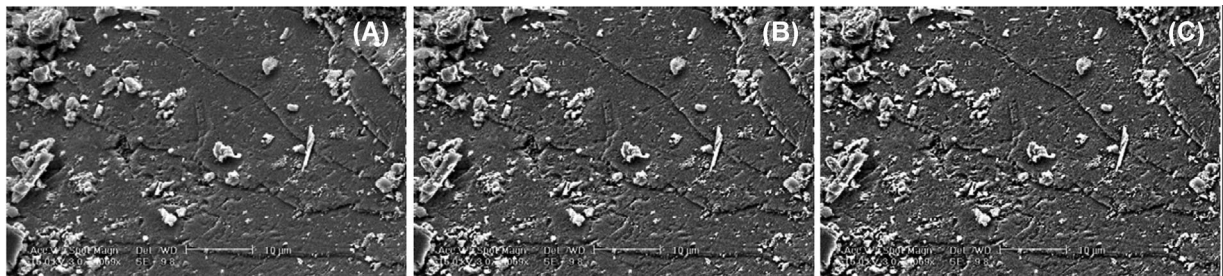


Fig. 13. Enhanced results of the proposed algorithm using different weights and scale number  $n = 3$  on one example mineral image. (A) Enhanced results with weights  $w_1 = w_2 = 0.5$ ; (B) Enhanced results with weights  $w_1 = w_2 = 1.0$ ; (C) Enhanced results with weights  $w_1 = w_2 = 1.5$ .

is not the largest in each figure, it takes the second place at all the figures. This indicates that the proposed algorithm indeed performs effectively for enhancing image details and spatial information while suppressing the produced noise, which gives the effective overall performance and would be useful for mineral image enhancement.

Using the sequential index of algorithms on different measures for the overall performance comparison is an appropriate and widely used way in image enhancement (Mukhopadhyay

& Chanda, 2000). A small value of the total value of the sequential indexes indicates a good overall performance of the corresponding algorithm. To clearly show the overall performance on these measures, we show the sequential index of each algorithm on each measure following the values of each measure in Table 1 (from the largest value to the smallest value). The total of the sequential index of each algorithm on all the measures is shown in the final row of Table 1. Table 1 shows that the total value of the sequential indexes of the

**Table 1.** Sequential indexes of the algorithms corresponding to each measure.

	The proposed algorithm	CTO	MSM	WF	HE	CLAHE
PSNR	2	1	6	5	4	3
SF	2	4	1	3	5	6
MG	2	4	1	3	6	5
Total	6	9	8	11	15	14

proposed algorithm is the smallest one, which indicates that the proposed algorithm has good overall performance comparing with other algorithms. Therefore, the proposed algorithm performs effectively for mineral image detail enhancement, spatial information enhancement, and noise suppression, which could be used for the further mineral image analysis.

To show the effects of the parameters, the enhanced results of the proposed algorithm using different parameters on one example mineral image corresponding to the original mineral image in Figure 1 are shown in Figures 12 and 13. Figure 12 lists the enhanced results by the proposed algorithm with different scale numbers and weights  $w_1 = w_2 = 1.0$ . Note that (A), (B) and (C) are the enhanced results with scale numbers  $n = 3, 4$  and  $5$ , respectively. Figure 12 shows that the difference between these results is not large. Usually, using larger scale number will extract more image features for mineral image enhancement, which may be more useful for mineral image enhancement. However, using very large scale number may over enhance some bright regions (Fig. 12C with scale number  $n = 5$ ), and the calculation time would be increased. So, there is no need to use very large scale number. Figure 12(A) shows that the result with scale number  $n = 3$  is effective and the result image is clear.

Figure 13 lists the enhanced results by the proposed algorithm with different weights and scale number  $n = 3$ . Note that (A), (B) and (C) are the enhanced results with weights  $w_1 = w_2 = 0.5$ ,  $w_1 = w_2 = 1.0$  and  $w_1 = w_2 = 1.5$ , respectively. Figure 13 shows that the difference between these results is also not large. And, if the weights  $w_1$  and  $w_2$  are large, some regions may be over enhanced and some noise may be produced (Fig. 13C with weights  $w_1 = w_2 = 1.5$ ), which will apparently change the grey scale distribution. So, there is no need to use large weight values. Figure 13(B) shows that using weights  $w_1 = w_2 = 1.0$  is simple and the result is clear and effective.

Therefore, in this paper, we use  $n = 3$ ,  $w_1 = w_2 = 1.0$ . Experimental results on different mineral images verified the effective performance of the proposed algorithm using these parameters.

Moreover, the proposed algorithm is fast and within the range of speeds that other algorithms produce.

Conclusions

In mineral microscopy imaging, obtaining unclear images is common. So, it is very useful to enhance the unclear min-

eral images. To improve the usability of unclear image, an image enhancement algorithm should enhance image detail and clarity. Moreover, the grey scale distribution of the enhanced image should not be apparently changed compared with the original mineral image. To effectively enhance mineral image, an algorithm using opening and closing-based toggle operator is proposed in this paper. Opening and closing are used to identify the useful mineral image features through the specified toggle operator. Then, the identified bright and dark mineral image features are extracted through comparing the result of toggle operator and the original mineral image. Also, the multiscale theory using multiscale structuring elements is used to extract the multiscale image features at different scales of mineral image. Finally, the extracted image features are appropriately used to enhance the original mineral image through the strategy of enlarging the contrast between the bright and dark image features.

Because of the designed toggle operator using opening and closing and the specified selection rules, the useful image features are identified and extracted for mineral image enhancement. Especially, the important mineral image details are effectively extracted. Moreover, the multiscale theory ensures that the multiscale image features at multiscales of mineral images are extracted. And, the strategy of enlarging the contrast between the bright and dark image features makes the image clear and ensures that the grey scale distribution of the enhanced mineral image is not apparently changed. Therefore, the proposed algorithm performs well for mineral image enhancement.

Experimental results on different types of mineral images show that the performances of the proposed algorithm are effective. And, the comparisons with other algorithms suggest that the proposed algorithm performs better than some other algorithms for mineral image enhancement. So, the proposed algorithm could be used for different mineral image-based applications.

Acknowledgements

The author thanks the anonymous reviewers and the editor for their very constructive comments. This work is partly supported by the National Natural Science Foundation of China (61271023), open funding project of State Key Laboratory of Virtual Reality Technology and Systems, Beihang University (BUAA-VR-12KF-04), Program for New Century Excellent Talents in University, Fundamental Research Funds for the Central Universities (YWF-13-T-RSC-028, YWF-13-JQCJ-026) and Innovation Foundation of AVIC.

References

Arianna, M., Marcello, S., Roberto, L., Manuela, F. & Federica, C. (2008). Mammographic images enhancement and denoising for breast cancer



- detection using dyadic wavelet processing. *IEEE Trans. Instrum. Meas.* **57**, 1422–1430.
- Aslantas, V. & Kurban, R. (2009). A comparison of criterion functions for fusion of multi-focus noisy images. *Opt. Commun.* **282**, 3231–3242.
- Bai, X., Sun, C. & Zhou, F. (2009). Splitting touching cells based on concave points and ellipse fitting. *Pattern Recognit.* **42**, 2434–2446.
- Bai, X. & Zhou, F. (2010a). Analysis of new top-hat transformation and the application for infrared dim small target detection. *Pattern Recognit.* **43**, 2145–2156.
- Bai, X. & Zhou, F. (2010b). Analysis of different modified top-hat transformations based on structuring element constructing. *Signal Process.* **90**, 2999–3003.
- Bai, X. & Zhou, F. (2011). Multiscale toggle contrast operator based mineral image enhancement. *J. Microsc.* **243**, 141–153.
- Bai, X., Zhou, F. & Xue, B. (2011). Fusion of infrared and visual images through region extraction by using multi scale center-surround top-hat transform. *Opt. Express* **19**, 8444–8457.
- Bruce, F. & Eric L.S. (1999). Adaptive nonlocal filtering: a fast alternative to anisotropic diffusion for image enhancement. *IEEE Trans. Pattern Anal. Mach. Intell.* **21**, 42–48.
- Carter, D., Scully, A., Hatton, P., Davies, R. & Aaron, J. (2000). Cryopreservation and image enhancement of juvenile and adult dentine mineral. *Histochem. J.* **32**, 253–261.
- Cheng, Q., Jing, L. & Panahi A. (2006). Principal component analysis with optimum order sample correlation coefficient for image enhancement. *Int. J. Remote Sens.* **27**, 3387–3401.
- Dorini, L. & Leite, N. (2007). A scale-space toggle operator for morphological segmentation. In *Proceedings of the 8th International Symposium on Mathematical Morphology*, pp. 101–112. Rio de Janeiro.
- Farzam, F., Mohammad, B.M., Seyed, A.M. & Martin, T.H. (2000). A new fuzzy logic filter for image enhancement. *IEEE Trans. Syst. Man Cybern.* **30**, 110–119.
- Foracchia, M., Grisan, E. & Ruggeri, A. (2005). Luminosity and contrast normalization in retinal images. *Med. Image Anal.* **9**, 179–190.
- Fürhapter, S., Jesacher, A., Bernet, S. & Ritsch-Marte, M. (2005). Spiral phase contrast imaging in microscopy. *Opt. Express* **13**, 689–694.
- Guy, G., Nir, S. & Yehoshua, Y.Z. (2004). Image enhancement and denoising by complex diffusion processes. *IEEE Trans. Pattern Anal. Mach. Intell.* **26**, 1020–1036.
- Hayit, G., Charles, H.A. & Sofia, A. (2000). Image enhancement by non-linear extrapolation in frequency space. *IEEE Trans. Image Process.* **9**, 1035–1048.
- Huang, K., Wang, Q. & Wu, Z. (2006). Natural color image enhancement and evaluation algorithm based on human visual system. *Comput. Vis. Image Underst.* **103**, 52–63.
- Jackway, P. & Deriche, M. (1996). Scale-space properties of the multiscale morphological dilation-erosion. *IEEE Trans. Pattern Anal. Mach. Intell.* **18**, 38–51.
- Li, Y., Lu, A., Ding H., Zeng C., Yan Y., Wang X. & Wang C. (2012). Synergistic interaction between electricigens and natural pyrrhotite to produce active oxygen radicals. *Geomicrobiol. J.* **29**, 264–273.
- Maragos, P. (2005). Morphological filtering for image enhancement and feature detection. In *The Image and Video Processing Handbook* (ed. by A.C. Bovik), pp. 135–156. Elsevier Academic Press, Amsterdam, The Netherlands.
- Mukhopadhyay, S. & Chanda, B. (2000). A multiscale morphological approach to local contrast enhancement. *Signal Process.* **80**, 685–696.
- Oliveira, M. & Leite, N. (2008). A multiscale directional operator and morphological tools for reconnecting broken ridges in fingerprint images. *Pattern Recognit.* **41**, 367–377.
- Peli, E., Lee, E., Trempe, C. & Buzney, S. (1994). Image enhancement for the visually impaired: the effects of enhancement on face recognition. *J. Opt. Soc. Am.* **11**, 1929–1939.
- Poulidakos, L.D. & Partl, M.N. (2010). Investigation of porous asphalt microstructure using optical and electron microscopy. *J. Microsc.* **240**, 145–154.
- Pradham, P., Younan, N. & King, R. (2008). Concepts of image fusion in remote sensing applications, In *Image Fusion: Algorithms and Applications* (ed. by T. Stathaki, T.), pp. 391–428. Academic Press, Great Britain.
- Schavemaker, J., Reinders, M., Gerbrands, J. & Backer, E. (2000). Image sharpening by morphological filtering. *Pattern Recognit.* **33**, 997–1012.
- Serra, J. (1988). Toggle mappings. *Technical Report N-18/88/MM*, Centre de Morphologie Mathématique, ENSMP, Fontainebleau, France.
- Sheet, D., Pal, S., Chakraborty, A., Chatterjee, J. & Ray, A. (2010) Visual importance pooling for image quality assessment of despeckle filters in Optical Coherence Tomography. In *Proceedings of International Conference on Systems in Medicine and Biology*, pp. 102–107. IIT Kharagpur, India.
- Soille, P. (2003). *Morphological Image Analysis-Principle and Applications*. Springer, Germany.
- Sos, S.A., Karen, P. & Artyom, M.G. (2001). Transform-based image enhancement algorithms with performance measure. *IEEE Trans. Image Process.* **10**, 267–382.
- Tang, B., Sapiro, G. & Caselles, V. (2001). Color Image Enhancement via chromaticity diffusion. *IEEE Trans. Image Process.* **10**, 701–707.
- Truc, P.T.H., Md, A.U.K., Lee, Y., Lee, S. & Kim, T. (2009). Vessel enhancement filter using directional filter bank. *Comput. Vis. Image Underst.* **113**, 101–112.
- Wan, Y. & Shi, D. (2007). Joint exact histogram specification and image enhancement through the wavelet transform. *IEEE Trans. Image Process.* **16**, 2245–2250.
- Yang, G.Z. & Hansell, D.M. (1997). CT image enhancement with wavelet analysis for the detection of small airways disease. *IEEE Trans. Med. Imaging* **16**, 953–961.
- Yang, C., Lu, L., Lin, H., Guan, R., Shi, X. & Liang, Y. (2008). A fuzzy-statistics-based principal component analysis (FS-PCA) method for multispectral image enhancement and display. *IEEE Trans. Geosci. Remote Sens.* **46**, 3937–3947.
- Yew, E. & Sheppard, C. (2006). Effects of axial field components on second harmonic generation microscopy. *Opt. Express* **14**, 1167–1174.
- Youngsik, C. & Raghu, K. (1997). A robust approach to image enhancement based on fuzzy Logic. *IEEE Trans. Image Process.* **6**, 808–825.